

# Links between jellyfish and microbes in a jellyfish dominated fjord

Lasse Riemann<sup>1,\*</sup>, Josefin Titelman<sup>2</sup>, Ulf Båmstedt<sup>2,3</sup>

<sup>1</sup>Department of Natural Sciences, Kalmar University, 39182 Kalmar, Sweden

<sup>2</sup>Department of Biology, University of Bergen, PO Box 7800, 5020 Bergen, Norway

<sup>3</sup>Umeå Marine Science Centre, University of Umeå, Norrbyn, 91020 Hörnefors, Sweden

**ABSTRACT:** Research on the impact of mass aggregations of jellyfish on foodweb structure has mainly focused on trophic control of copepods and fish larvae, while impacts on lower trophic levels have received little attention. Jellyfish release nutrients and dissolved organic matter through their activities. Hence, both direct and cascading impacts of jellyfish on the bacterial community are conceivable. In the Norwegian Lurefjorden, the abundance of the deepwater scyphomedusa *Periphylla periphylla* reaches concentrations much higher than in any other area investigated. We used Lurefjorden as a model system to examine effects of high jellyfish biomass on the microbial planktonic foodweb, and targeted bacterial activity and community composition in relation to the distribution of *P. periphylla* as monitored using a Remotely Operated Vehicle. *P. periphylla* performed pronounced diel vertical migrations; however, no significant diel effects on microbial activity were observed in surface waters. Surface waters were characterized by a high biomass of mesozooplankton. Integrating over 24 h, the highest jellyfish biomass was found at 200 to 300 m depth. This concurred with elevated total organic carbon, bacterial production and ectoenzymatic activities. Analysis of bacterioplankton community composition by denaturing gradient gel electrophoresis (DGGE) and 16S rDNA sequencing revealed that specific phylotypes related to Bacteroidetes and to  $\delta$ -Proteobacteria were found with depth. Overall, phylotypes related to Bacteroidetes dominated the bacterial community. Our results indicate that *P. periphylla* has a structuring impact on the pelagic deep-water microbial community in Lurefjorden. We suggest that jellyfish proliferations may also be quantitatively important for lower trophic levels of the pelagic foodweb.

**KEY WORDS:** *Periphylla periphylla* · Jellyfish · Bacteria · Community composition · DGGE

Resale or republication not permitted without written consent of the publisher

## INTRODUCTION

Gelatinous zooplankton occur throughout the water column in all of the world's oceans. When numerous, jellyfish commonly disrupt fisheries, tourism and coastal industries. Whether the frequency and extent of such blooms have increased worldwide remains disputable; however, at local scales numerous examples exist (Mills 2001, Lynam et al. 2004). The ecological impact of jellyfish proliferations on foodweb structure and dynamics may at times be significant. For example, large jellyfish populations may directly control larval fish (Purcell & Arai 2001) and zooplankton pop-

ulations (Olesen 1995). Reports on impact of jellyfish on lower trophic levels are few however, despite the possibility of both indirect cascade effects (Stibor et al. 2004) and direct substrate generation (Hansson & Norrman 1995). Their voracious feeding activity on zooplankton and fish may potentially elicit cascading effects in pelagic foodwebs affecting trophic levels down to microbes. For instance, Priddle et al. (2003) demonstrated in the northern Scotia Sea that variations in krill biomass change the relative impact of krill and copepods on phytoplankton, which in turn regulates nutrient cycles. Stibor et al. (2004) examined cascading effects on phytoplankton and found that jellyfish con-

\*Email: lasse.riemann@hik.se

sistently reduced copepod biomass while the net effect on algal biomass depended on initial cell size, and their susceptibility to copepod grazing. Altered phytoplankton size distribution likely influences the release of organic carbon from algal cells (Bjørnsen 1988), which in turn, affects bacterial growth. Jellyfish biomass may also stimulate bacterial growth directly through release of nutrients (Schneider 1989, Nemazie et al. 1993) and bio-available dissolved organic matter (DOM) (Hansson & Norrman 1995, Titelman et al. 2006, this volume). Hence, by modifying carbon and nutrient conditions jellyfish may potentially influence microbial community composition (Martinez et al. 1996), however this has not yet been examined *in situ*.

Most jellyfish may undergo rapid population increases, as well as aggregations, in response to changes in food availability and the physical environment. Naturally, the irregularity and unpredictability of these proliferations constrain studies of their impact on the concomitant planktonic community. In a few Norwegian fjords, the perennial deepwater scyphomedusa *Periphylla periphylla* abounds year-round (Youngbluth & Båmstedt 2001) forming lasting mass-occurrences with average concentrations of  $\sim 0.4 \text{ m}^{-3}$  in the deep basin of Lurefjorden (integrating over the entire water column, Sørnes 2005). Such concentrations are several orders of magnitude greater than in the open ocean (Youngbluth & Båmstedt 2001).

Here, Lurefjorden was used as a model system to examine the effects of a persistently high jellyfish biomass on the planktonic foodweb and, especially, on bacterial activity and community composition. We hypothesized that the diel vertical migration of jellyfish (Youngbluth & Båmstedt 2001) would cause an accumulation of jellyfish biomass near the surface at night and at depth during the day, which through the release of bioavailable dissolved organic carbon and nutrients, would stimulate bacterial activity (Schneider 1989, Nemazie et al. 1993, Hansson & Norrman 1995) near the surface and at depth at day and night, respectively. We also hypothesized that the strong vertical gradient in jellyfish biomass would lead to changes in bacterial community composition with depth.

## MATERIALS AND METHODS

We examined the potential impact of the jellyfish biomass and its tremendous diel biomass-movement on planktonic microbial activity and biomass in the deep basin (max. depth 439 m) of Lurefjorden, Western Norway, (60° 42.73' N, 05° 05.60' E) on April 22 to 23, 2004. We conducted a 24 h study at 5 m depth, where *Periphylla periphylla* are completely absent during daytime, but abundant at night, as well as a vertical pro-

file study to document changes during day and night conditions. The hydrography of Lurefjorden and the biology of *P. periphylla* is described in detail elsewhere (Eiane et al. 1999, Youngbluth & Båmstedt 2001).

For the 24 h study, water samples were obtained from 5 m depth with 10 l Niskin bottles attached to a rosette sampler every 3 h between 04:00 h April 22 and 04:00 h April 23. The vertical profiles were performed at daytime (13:00 h) on April 22 and at nighttime (01:00 h) on April 23, where bottle samples were taken at 5, 25, 50, 100, 200 and 300 m depth. The water was transferred to 10 l acid-washed containers and sampled for chlorophyll *a* (chl *a*), nutrients, total organic carbon (TOC), bacterial production, aminopeptidase and phosphatase activities, bacterial community DNA, and bacterial, viral, ciliate and copepod abundance. Temperature and salinity were measured simultaneously during each sampling. The distribution and biomass of *Periphylla periphylla* was assessed from video profiles from a Remotely Operated Vehicle (ROV) and net sampling, respectively.

***Periphylla periphylla*.** Methods and equipment associated with sampling *P. periphylla* are described in detail elsewhere (Youngbluth & Båmstedt 2001, Sørnes 2005) and therefore summarized only briefly here. Vertical distribution in the entire water column was assessed from 6 video profiles on April 22–23 by the ROV 'Aglantha' in the deep basin (320 to 439 m depth). The recordings were conducted at a ROV descent rate of  $\sim 0.5 \text{ m s}^{-1}$ . The depth of each jellyfish was determined, and abundance was subsequently integrated in 10 m depth intervals. To convert data to concentrations, we multiplied the vertical distance traveled with empirically determined horizontal surface areas of 2.31 and 6.09  $\text{m}^2$ , determined for small (2 cm coronal diameter) and large (10 cm coronal diameter) *P. periphylla* (Youngbluth & Båmstedt 2001). Following Sørnes (2005) we report concentrations as ranges using the 2 area factors, as jellyfish sizes cannot be accurately determined with this video set-up. We complimented these data with direct surface counts at night.

Depth integrated *Periphylla periphylla* biomass was obtained from vertical net tows (2 m mouth diameter, 12.5 m long, 3 to 1 mm graded mesh size, plastic bag cod end) between the bottom and the surface at a rate of  $\sim 6 \text{ m min}^{-1}$ . The diameter of all animals was measured to the nearest mm and their wet weight determined to the nearest 0.1 g.

**Chl *a*, nutrients and total organic carbon (TOC).** Duplicate 1 l samples were filtered and chl *a* extracted in ethanol and measured using a Turner design 10-AU fluorometer (excitation 340 to 500 nm band pass; emission >665 nm cut-off) calibrated with a standard chl *a* solution (Sigma). For nitrate/nitrite, ammonia and phosphate, three 12 ml samples were filtered through

glass fiber filters (Whatman GF/F) into 15 ml polypropylene tubes and frozen until analysis using a Bran & Luebbe TRAACS 800 autoanalyzer and standard seawater methods (Grasshoff et al. 1983). For TOC, duplicate 12 ml samples were frozen in 15 ml polypropylene tubes and analyzed using a Shimadzu TOC-5000 high temperature catalytic oxidation instrument. Samples were acidified and sparged prior to analysis. Calculation of carbon concentrations was made with potassium hydrogen phthalate as standard substance.

**Ciliates.** For ciliate counts, 250 ml samples were fixed with Lugol's solution. Ciliates were enumerated under an inverted microscope using sedimentation chambers. Cell volumes ( $x$ ;  $\mu\text{m}^3$ ) were estimated from length and width measurements, and converted to carbon biomass ( $y$ ; pg C) using the relationship determined for protists:  $y = 0.216x^{0.939}$  (Menden-Deuer & Lessard 2000).

**Mesozooplankton.** Mesozooplankton from ~5 l were concentrated on a 45  $\mu\text{m}$  mesh, preserved in formalin (4% final) and measured and identified under a dissecting microscope. Prosome lengths (copepodids) and total lengths (nauplii) were converted to carbon weights using regressions in Rey-Rassat et al. (2004) (*Calanus* spp.), Sabatini & Kiørboe (1994) (*Oithona similis*, also used for *Oncaea* spp.), and Berggreen et al. (1988) (*Acartia tonsa*, used for all other species and for nauplii).

**Bacterial and viral abundance.** Aliquots of 45 ml were fixed with 0.2  $\mu\text{m}$  filtered formalin (2% final) and stored at 4°C for 1 mo before bacterial and viral enumeration. Bacteria were stained with SYTO 13 (Molecular Probes) and counted on a FACSCalibur flow cytometer (Becton Dickinson) (Gasol & del Giorgio 2000) using fluorescent beads (True counts, Becton Dickinson) as standards. For viral counts, 5 to 7 ml aliquots were filtered onto 0.02  $\mu\text{m}$  Anodisc filters (Whatman), stained with SYBR Green I (Molecular probes), and mounted in glycerol/p-phenylenediamine (Noble & Fuhrman 1998). More than 200 viruses filter<sup>-1</sup> (or >15 fields filter<sup>-1</sup>) were counted at 1250 $\times$  using epifluorescence microscopy (Zeiss Axioplan). Duplicate filters were counted on 3 occasions. The coefficient of variation between duplicate filters was on average 7%. The bacterial and viral counts are probably conservative because of the preservation in formalin (e.g. Wen et al. 2004).

**Bacterial production.** Bacterial production was measured by [<sup>3</sup>H]-thymidine incorporation (Fuhrman & Azam 1982). For each sample, triplicate aliquots (10 ml) and a fixed blank were incubated with [methyl-<sup>3</sup>H]-thymidine (10 nM final, Amersham Pharmacia Biotech) in polyethylene vials in a water bath with flowing surface seawater on deck for ca. 1 h. Samples with 5%

trichloroacetic acid added prior to the addition of [<sup>3</sup>H]-thymidine were used as blanks. Samples were filtered onto 0.2  $\mu\text{m}$  mixed cellulose ester filters (Advantec MFS), rinsed carefully with ice-cold 5% trichloroacetic acid, and counted by liquid scintillation spectrometry. Bacterial carbon production was calculated using  $1.1 \times 10^{18}$  cells mol<sup>-1</sup> thymidine incorporated (Riemann et al. 1987) and a carbon-to-cell ratio of 20 fg C bacterium<sup>-1</sup> (Lee & Fuhrman 1987).

**Hydrolytic ectoenzyme activities.** Triplicate 4 ml samples were incubated with fluorogenic substrates (methylumbelliferyl [MUF] and amino-methylcoumarin [AMC] derivatives, Sigma) to determine potential hydrolysis rates. The substrates used (and enzymes assayed) were L-leucine-AMC (aminopeptidase) and MUF-phosphate (alkaline phosphatase). Substrate hydrolysis rates were measured with a Turner TD-700 fluorometer using heat-killed samples as controls. The fluorometer was calibrated with standard solutions of MUF and AMC (Sigma) and potential activities at 200  $\mu\text{M}$  substrate concentration were measured.

**DNA filtration and extraction.** For DNA extraction, 2 to 3 liters of water was filtered through a 0.22  $\mu\text{m}$  Sterivex capsule filter (Millipore) via a peristaltic pump. Filters were frozen at -20°C until extraction. DNA was extracted from filters using an enzyme/phenol-chloroform protocol as described in Riemann et al. (2000), but with a few modifications: a 30 min lysozyme treatment (5 mg ml<sup>-1</sup>, final) and an overnight proteinase K (2 mg ml<sup>-1</sup> final) treatment at 55°C as optimized by Boström et al. (2004). DNA was re-suspended in TE (10 mM Tris, 1 mM EDTA, pH 8.0) and quantified fluorometrically (PicoGreen; Molecular Probes).

**PCR-amplification, DGGE and 16S rDNA sequencing.** Bacterial 16S rDNA was amplified using a Bacterial primer complementary to position 341 to 358 with a 40 bp GC-clamp (Muyzer et al. 1993) and a universal primer complementary to position 907 to 927 (Muyzer et al. 1998). PCR reactions (75  $\mu\text{l}$ ) contained 1X PCR buffer with MgCl<sub>2</sub> (Roche), 0.8 mM deoxynucleotide triphosphates, 0.5  $\mu\text{M}$  of each primer,  $\approx 7.5$  ng of template DNA, and 1.5 units of *Taq* polymerase (Roche). Initial denaturation was at 95°C for 2 min followed by a thermal cycling program as follows: denaturation for 30 s at 94°C; annealing for 30 s at an initial 63°C, decreasing 1°C every 2 cycles to a final of 53°C; extension for 90 s at 72°C. Ten cycles were run at 53°C for a total of 30 cycles followed by final 7 min incubation at 72°C. A negative control, in which the template was replaced by an equivalent volume of sterile water, was included in each batch of PCR reactions. Quality and size of PCR products were verified by agarose gel electrophoresis.

Duplicate 75  $\mu\text{l}$  PCR reactions were pooled, purified using the QIAquick Nucleotide Removal Kit (Qiagen),

and quantified fluorometrically. We analysed 60 ng of PCR product by DGGE using the D Gene System (Bio-Rad) at 60°C for 6 h at 150 V (Riemann & Middelboe 2002). DGGE bands were excised, eluted, re-amplified, and cloned (Riemann & Winding 2001). DGGE profiles of re-amplified, cloned DNA were used to check for heteroduplexes and to confirm the position of cloned bands relative to the original sample. Inserts were bi-directionally sequenced using the DYE-namic™ ET terminator cycle sequencing kit (Amersham Biosciences) and an ABI PRISM 377 sequencer (Applied Biosystems) as described by the manufacturer. Sequences were aligned to known sequences using BLAST (Altschul et al. 1990) and analyzed by the program Chimera Check (Cole et al. 2003). DGGE band sequences have been deposited in GenBank, using the abbreviations LUR 1 to 15 (LUR refers to Lurefjorden), under the accession numbers (in order) AY960276 to AY960290.

## RESULTS

### Vertical study

#### Basic parameters

The hydrography was characterized by stratification. Temperature decreased rapidly from 7 to 8°C near the surface to a minimum of 6°C below 100 m. Salinity increased from 31.5 at the surface to 33 below ~30 m.

Visual inspection of Figs. 1, 3 and 4 generally suggested no consistent or systematic differences between day and night profiles. We therefore tested for statistical differences between day and night profiles using paired Wilcoxon Signed-Ranks Tests. For variables where there were no significant differences between day and night, the 2 profiles were pooled before subsequent analyses. With the exception of ammonia ( $p = 0.028$ ), none of the other basic parameters differed significantly between day and night (all  $p$ -values  $> 0.05$ ) (Fig. 1).

Phosphate differed between depths (ANOVA on ranks,  $p < 0.001$ ), and generally increased from 0.1  $\mu\text{M}$  near the surface to 0.5  $\mu\text{M}$  at 200 to 300 m (Spearman's correlation,  $r = 0.891$ ,  $p = 0.001$ ). Ammonia did not differ significantly between depths (ANOVA on ranks,  $p = 0.255$ ) but ranged from ~0.8 to 0.9  $\mu\text{M}$  at 50 to 300 m to a peak of ~1.2  $\mu\text{M}$  at 25 m (Fig. 1B). Nitrite/nitrate concentrations were variable and differed between depths (ANOVA on ranks,  $p = 0.032$ ), increasing from ~0.5  $\mu\text{M}$  near the surface to ~4.5  $\mu\text{M}$  at 300 m (data not shown) (Spearman's correlation,  $r = 0.887$ ,  $p < 0.001$ ).

Phytoplankton biomass, proxied by chl *a*, differed between depths (ANOVA on ranks,  $p < 0.001$ ) decreasing from ~1.5  $\mu\text{g l}^{-1}$  near the surface to  $< 0.2 \mu\text{g l}^{-1}$

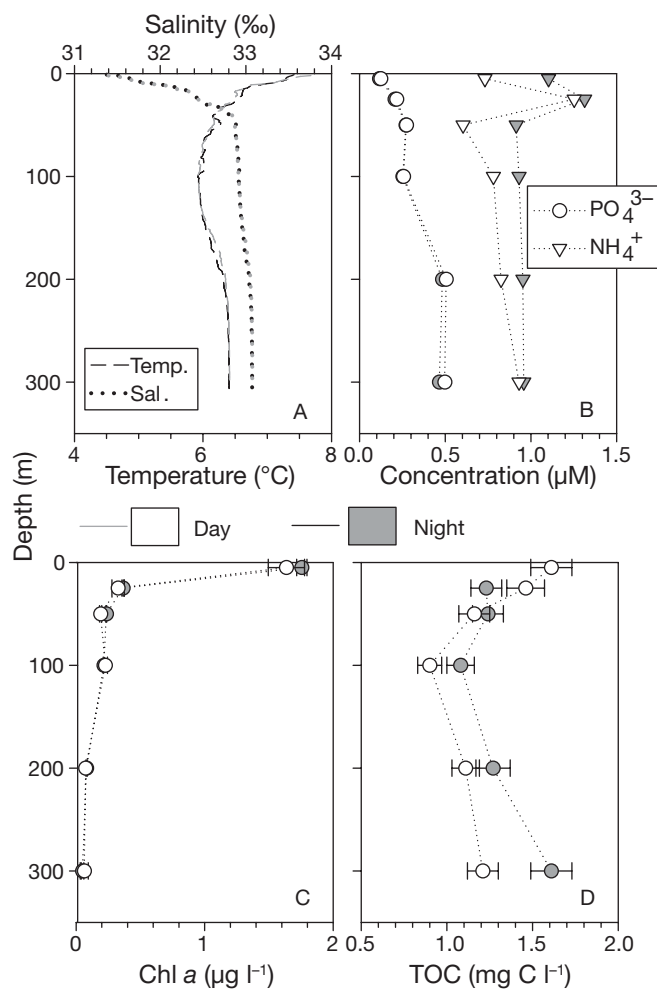


Fig. 1. Vertical distribution of (A) temperature and salinity, (B) nutrients, (C) chl *a*, and (D) total organic carbon (TOC), for day and night. Error bars are  $\pm$ SD based on duplicate samples for (C) chl *a*, and an 8% error averaged from 10 samples measured in duplicates for (D) TOC

below 50 m (Fig. 1C) (Spearman's correlation,  $r = -0.961$ ,  $p < 0.001$ ). Except for a few dinoflagellates, the phytoplankton community consisted almost exclusively of cryptophytes (*Plagioselmis* spp., *C. Legrand* pers. comm.) with a maximum concentration of 3800 cells  $\text{ml}^{-1}$  at 5 m (not shown).

Total organic carbon (TOC) was highest near the surface (~2  $\text{mg C l}^{-1}$ ), lowest (~1  $\text{mg C l}^{-1}$ ) at 100 m, and then increased to ~1.4  $\text{mg C l}^{-1}$  at 300 m (Fig. 1D). The fit of a quadratic polynomial to the plotted data statistically confirmed this visual impression of a mid depth minimum; the quadratic term was significant ( $p = 0.013$ ) yielding a TOC minimum at ~151 m (fit in Fig. 2D). Similarly, TOC concentrations and depth were negatively correlated from 5 to 100 m (Spearman's correlation,  $r = -0.899$ ,  $p = 0.003$ ) and positively correlated from 100 to 300 m depth ( $r = 0.786$ ,  $p = 0.032$ ).

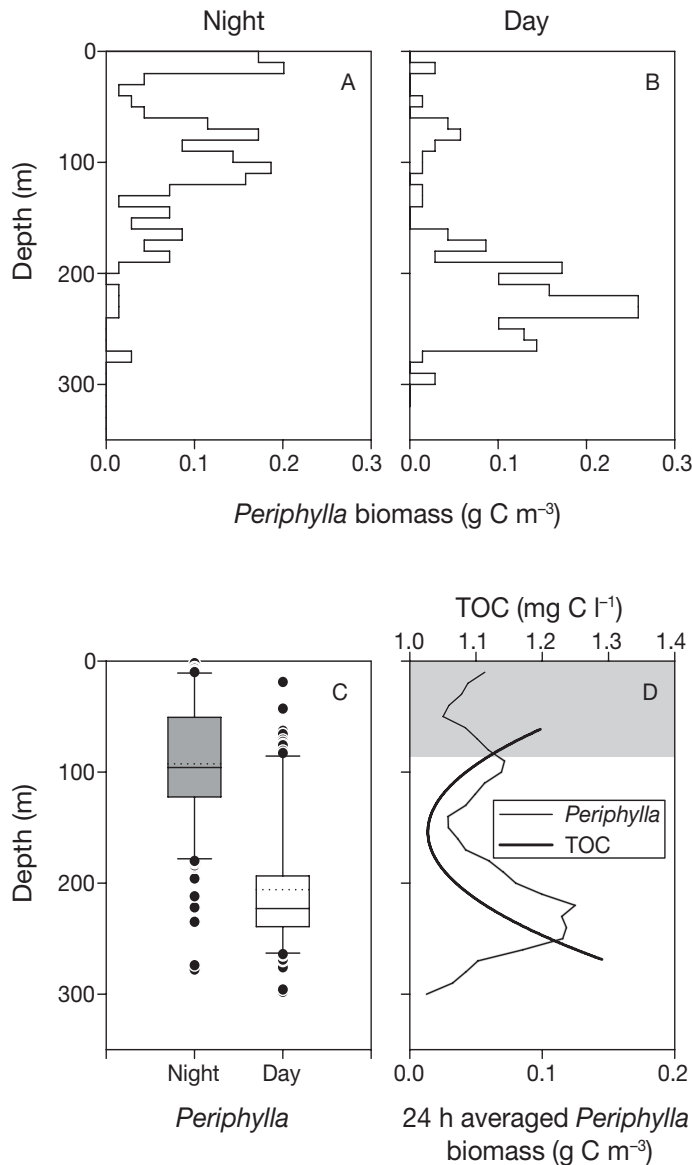


Fig. 2. *Periphylla periphylla*. Vertical distribution during night and day. (A & B) Biomass during night and day determined from ROV dives at (A) 21:55 to 22:27 h and (B) 10:31 to 10:58 h. Data were pooled in 10 m intervals. Counts were converted to concentrations by using the mean obtained from applying the 2 conversion factors (see 'Materials and methods'). Biomass was then calculated using a mean *P. periphylla* wet weight of 84.3 g (Table 1) and a conversion factor of  $0.571 \pm 0.194\%$  carbon per unit wet weight (mean  $\pm$  SD,  $n = 55$ , Båmstedt et al. unpubl.). (C) Box plots of individual depth distribution of *P. periphylla*. Boxes represent the 25th and 75th percentiles, whiskers the 5th and 95th percentiles. The median is indicated by the solid line, the mean by the stippled line, and outliers as circles. (D) 24 h integrated biomass of *P. periphylla* calculated from (A) & (B) by weighting with hours of daylight. Data are smoothed with a running average of 5 depth intervals. The line for TOC is the fit of a quadratic polynomial to the data in Fig. 1D. The fit is only shown for the depths where *P. periphylla* and TOC are correlated (see 'Results'). Grey shading indicates zone influenced by phyto- and zooplankton

### Biomass and distribution of *Periphylla periphylla*

The continuous profiles of *Periphylla periphylla* (Fig. 2) allowed for comparison of the depth distribution by day and night using a 2-sample Kolmogorov-Smirnov test. Day and night distributions differed significantly ( $p < 0.00001$ ). *P. periphylla* performed a pronounced diel vertical migration from a mean depth of  $92 \pm 61$  m at night to  $206 \pm 58$  m during the day (mean  $\pm$  SD) (Fig. 2C). Estimated biomass near the surface was  $0.2 \text{ g C m}^{-3}$  during the night, but  $0.2$  to  $0.3 \text{ g C m}^{-3}$  at 200 to 300 m depth during the day (Fig. 2A,B). As determined from ROV video profiles, the peak concentration was  $\sim 3.3\times$  the average concentrations (Table 1). This pattern was consistent in all profiles (data not shown). At midnight, surface counts of *P. periphylla* from deck revealed up to  $0.5 \text{ m}^{-2}$ ; no *P. periphylla* were observed at the surface during the day.

To compare the video-based depth profiles of *Periphylla periphylla* distribution with TOC distribution, sampled at discrete depths, average profiles were constructed for both variables. For *P. periphylla* a 24 h integrated depth profile was made by weighting the day and night depth profiles (Fig. 2A,B) with respect to light (15.25:8.75 h light:dark). This procedure revealed a local minimum of *P. periphylla* at  $\sim 130$  to  $160$  m (Fig. 2D), which coincided with the TOC minimum (Figs. 1D & 2D). Mean *P. periphylla* biomass ( $\text{g C l}^{-1}$ ) was subsequently calculated for depth intervals corresponding to the depths of TOC measurements (0–5, 5–25, 25–50, 50–100, 100–200 and 200–300 m). TOC values were first normalized to the highest value in each profile (day and night), where after an average TOC distribution was calculated for the same depth intervals as above. A Spearman's correlation analysis revealed no significant correlations between *P. periphylla* biomass and TOC, when including data for the entire water column pooled in this way ( $r = 0.600$ ,  $p = 0.104$ ,  $n = 6$ ). However, the TOC concentration in surface waters is influenced by phytoplankton and mesozooplankton activities (Figs. 1, 2D & 3), and the 24 h integrated *P. periphylla* profile has 2 distinct peaks (Fig. 2D). It is therefore relevant to compare different sections of the water column separately. Visual inspection of Fig. 2D suggests that *P. periphylla* distribution and TOC are well correlated between  $\sim 80$  m and  $\sim 260$  m, but not at depths influenced by phytoplankton and mesozooplankton, and below the largest *P. periphylla* peak (260 to 300 m). This relationship was confirmed by a Spearman's correlation analysis of 20 m depth interval raw data for both *P. periphylla* and TOC. The TOC subdivisions were constructed by interpolation from the discrete sampling depths (cf. Fig. 1D). TOC and *P. periphylla* concentrations were positively

Table 1. *Periphylla* concentration as determined from ROV transects and MIK nets in the deep basin of Lurefjorden, April 20 to 23, 2004. All data are mean  $\pm$  SD. Data from ROV profiles are given as a range using the 2 conversion factors (see 'Materials and methods')

	ROV (n = 6)		MIK (n = 2)
	6.09 m <sup>2</sup>	2.31 m <sup>2</sup>	
Integrated concentration, 0 m to bottom (ind. m <sup>-3</sup> )	0.077 $\pm$ 0.020	0.202 $\pm$ 0.054	0.053 $\pm$ 0.008
Max. concentration at any 10 m depth interval (ind. m <sup>-3</sup> )	0.285 $\pm$ 0.073	0.750 $\pm$ 0.193	–
Individual wet weight (kg) (n = 122)	–	–	0.084 $\pm$ 0.121

correlated between 80 and 260 m ( $r = 0.667$ ,  $p = 0.025$ ,  $n = 9$ ). When including depths below the *P. periphylla* peak (i.e. >260 m) or above 80 m the correlations break down.

### Biomass and distribution of micro- and mesozooplankton

There were no significant differences between day and night profiles for ciliates or copepods (paired Wilcoxon Signed Ranks Tests, all  $p$ -values > 0.05). Ciliate biomass differed between depths (ANOVA on ranks,  $p = 0.001$ ), and was generally negatively correlated with depth decreasing from  $\sim 1 \mu\text{g C l}^{-1}$  near the surface (Fig. 3A) (Spearman's correlation,  $r = -0.961$ ,  $p < 0.001$ ). However, ciliates contributed insignificantly to total biomass (cf. Figs. 2 & 3). The mesozooplankton community was dominated by copepods, which were abundant near the surface and at 200 to 300 m ( $\sim 10$  copepods  $\text{l}^{-1}$ , Fig. 3B). The copepod

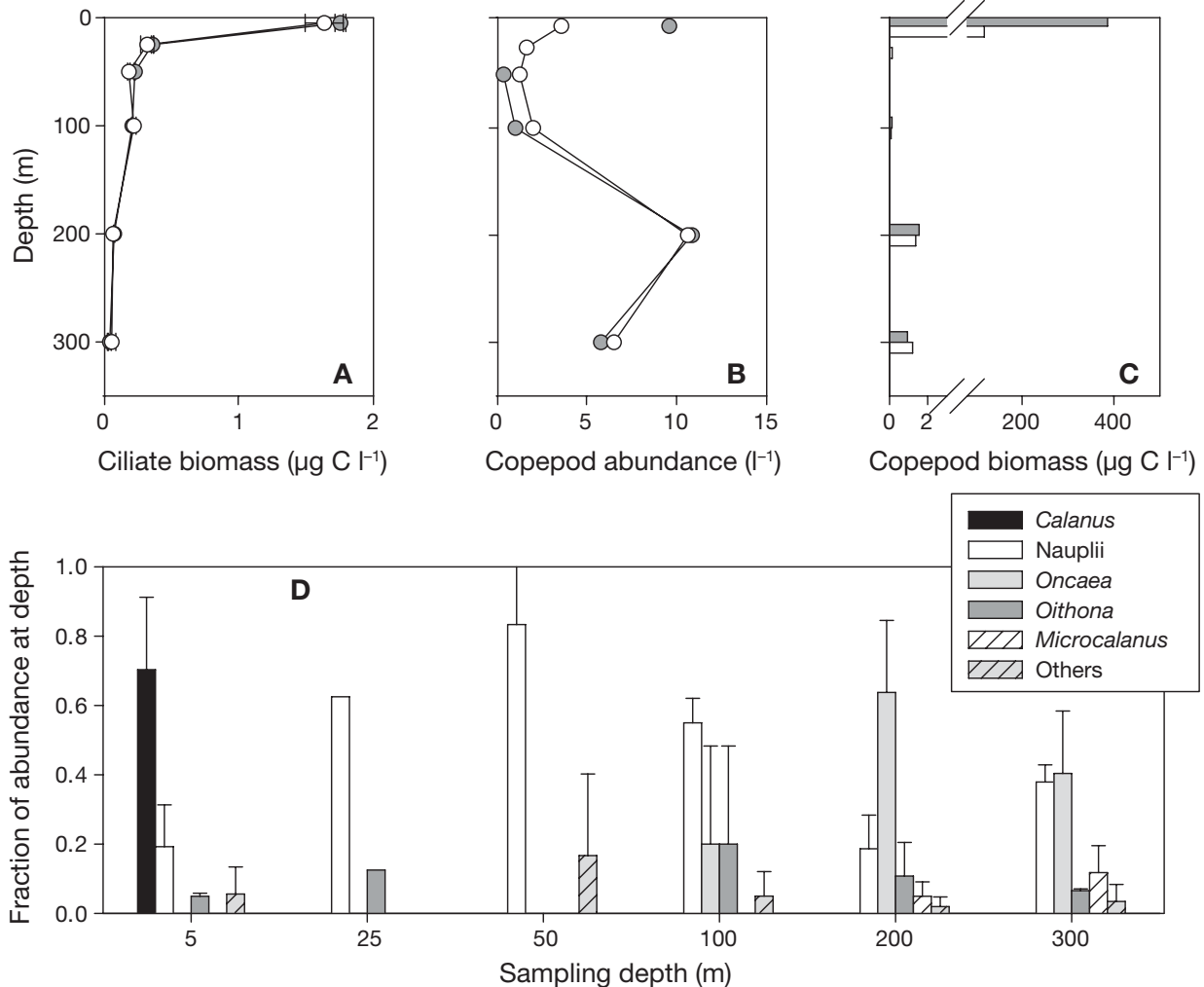


Fig. 3. Vertical profiles of micro- and mesozooplankton during night and day. (A) Ciliate biomass. (B & C) Copepod abundance and biomass. (A–C) Light and dark symbols indicate day and night samplings, respectively. (D) Taxonomic composition of mesozooplankton as a function of depth. Non-copepod plankton are included in the 'others' category. The composition is calculated as the fraction at depth, such that the total fraction at each depth adds up to 1. Error bars are  $\pm$ SD

community was dominated numerically by *Calanus* spp. copepodite stages near the surface and by small copepods (mainly *Oncaea* spp., *Oithona* spp. and nauplii) at 200 to 300 m depth (Fig. 3D). Copepod biomass differed between depths (ANOVA on ranks,  $p < 0.001$ ). *Calanus* spp. dominated the copepod biomass, as evident from the  $\geq 100$ -fold higher values at 5 m relative to the other depths. The many nauplii and small copepods at depth contributed comparatively little to the biomass (Fig. 3C).

#### Microbial abundance and activity

Neither bacterial abundance nor production differed between day and night (paired Wilcoxon Signed Ranks Test,  $p = 0.172$  and  $p = 0.463$ , respectively). Bacterial abundance differed between depths (ANOVA on ranks,  $p = 0.001$ ) and generally decreased with depth from  $\sim 1.0 \times 10^6 \text{ ml}^{-1}$  near the surface to  $\sim 0.2$  to  $0.3 \times 10^6 \text{ ml}^{-1}$  at 200 to 300 m depth (Fig. 4A) (Spearman's correlation,  $r = -0.961$ ,  $p < 0.001$ ).

Bacterial production was highest near the surface ( $\sim 2 \mu\text{g C l}^{-1} \text{ d}^{-1}$ ), lowest at 50 to 100 m ( $0.1$  to  $0.3 \mu\text{g C l}^{-1} \text{ d}^{-1}$ ), below which it increased slightly down to 300 m (Fig. 4B). This visual impression of minimum production at mid-depth was statistically confirmed by a quadratic polynomial fit to the ranked data; the quadratic term (i.e. the minimum) was significant ( $p = 0.026$ ) (not shown). Similarly, production from 5 to 100 m was negatively correlated with depth (Spearman's correlation,  $r = -0.927$ ,  $p < 0.001$ ), while production between 100 and 300 m was positively correlated with depth ( $r = 0.956$ ,  $p = 0.001$ ). In addition, bacterial production was positively correlated with TOC over the entire water column (Spearman's correlation,  $r = 0.706$ ,  $p = 0.008$ ).

While aminopeptidase activities did not differ between day and night (paired Wilcoxon Signed Ranks Test,  $p = 0.463$ ), phosphatase activity did ( $p = 0.028$ ). Ecto-enzymatic activities apparently mirrored the pattern of bacterial production (Fig. 4) and TOC (Fig. 1) with a minimum at mid-depth. Phosphatase and aminopeptidase activities were highest near the surface ( $\sim 10$  and  $\sim 50 \text{ nM h}^{-1}$ , respectively), lowest between 50 and 100 m ( $\sim 2$  and  $\sim 20 \text{ nM h}^{-1}$ , respectively), and increasing down to 300 m (Fig. 4C,D). The quadratic term (i.e. the minimum) of quadratic polynomial fits to the ranked data versus depth was significant for aminopeptidase ( $p = 0.004$ ), but not for phosphatase ( $p = 0.052$ ). Separate correlations between enzyme activity and depth, for the depth ranges 5 to 100 m and 100 to 300 m also suggested an activity minimum at mid-depth for aminopeptidase (Spearman's correlation, 5 to 100 m:  $r = -0.976$ ,  $p < 0.001$ ; 100 to 300 m:  $r = 0.956$ ,  $p = 0.001$ ) and phosphatase (5 to 50 m:  $r = -0.849$ ,  $p = 0.016$ ; 50 to

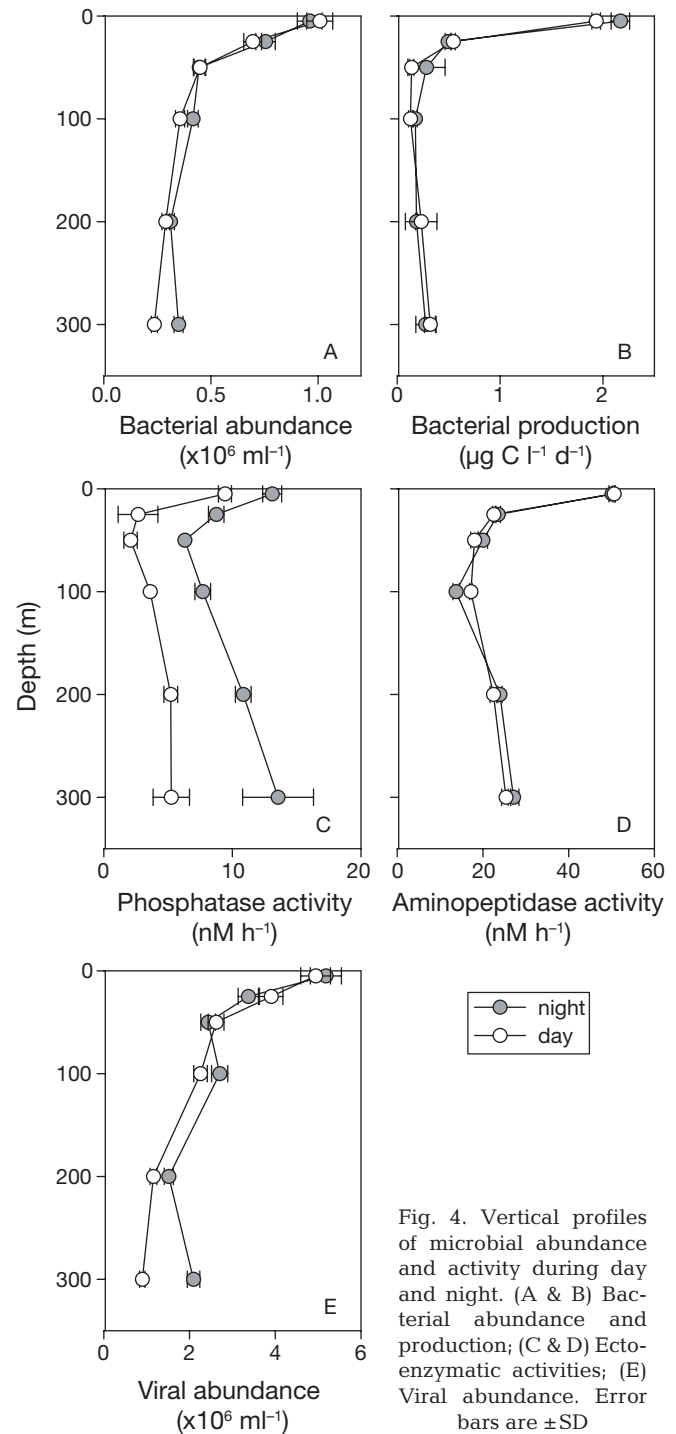


Fig. 4. Vertical profiles of microbial abundance and activity during day and night. (A & B) Bacterial abundance and production; (C & D) Ecto-enzymatic activities; (E) Viral abundance. Error bars are  $\pm$ SD

300 m:  $r = 0.732$ ,  $p = 0.019$ ). For phosphatase activity, which differed between day and night, data were normalized against the highest value in its respective profile, before the correlation analysis. The 2 enzyme activities were positively correlated with each other (Spearman's correlation,  $r = 0.664$ ,  $p = 0.004$ ). Both aminopeptidase and phosphatase activity were also

positively correlated with TOC over the entire water column (Spearman's correlation,  $r = 0.806$ ,  $p = 0.001$ , and  $r = 0.547$ ,  $p = 0.041$ , respectively). However, while bacterial production and aminopeptidase activity were significantly correlated (Spearman's correlation,  $r = 0.755$ ,  $p = 0.002$ ), the correlation was not significant for phosphatase activity ( $r = 0.455$ ,  $p = 0.074$ ).

Viral abundance did not differ between day and night (Wilcoxon's paired rank test,  $p = 0.345$ ), but differed between depths (ANOVA on ranks,  $p = 0.001$ ). Viral abundance was negatively correlated with depth (Spearman,  $r = -0.933$ ,  $p < 0.001$ ) decreasing from  $\sim 5 \times 10^6 \text{ ml}^{-1}$  near the surface to  $\sim 1\text{--}2 \times 10^6 \text{ ml}^{-1}$  at 200 to 300 m (Fig. 4E). Viral abundance was positively correlated with both bacterial abundance (Spearman,  $r = 0.965$ ,  $p < 0.001$ , 1-tailed) and bacterial production (Spearman,  $r = 0.545$ ,  $p = 0.033$ ) over the entire water column.

#### Bacterial community composition

We used PCR-DGGE analysis of 16S rDNA to examine bacterial community composition. Ideally, this analysis provides a graphical 'fingerprint' of the bacterial community composition. Potential biases inherent in the DNA extraction and PCR-DGGE protocols are described elsewhere (Wintzingerode et al. 1997, Muyzer et al. 1998).

Only minor differences in the relative brightness of DGGE bands were detected when comparing fingerprints from day and night depth profiles, while no differences in the presence (or absence) of bands were discernible (data not shown). The relative brightness of bands changed with increasing depth, especially at 200 to 300 m (Fig. 5). The PCR-amplicons consisted of 9 to 23 discernible bands with a marked increase in the number of bands from the surface to deeper samples.

Fifteen different bands from the gel were excised, cloned and sequenced to obtain an impression of bacterial community composition. Bands from different depths with identical vertical positions in the gel had identical sequences (Band 10; Fig. 5). The sequenced amplicons were related to Bacteroidetes (47%), photosynthetic organisms (20%),  $\alpha$ - (13%),  $\delta$ - (13%) and  $\gamma$ -Proteobacteria (7%) (Fig. 5, Table 2). Except for 2 amplicons related to Bacteroidetes (Bands 5 and 13), the amplicons were closely related to known sequences in the databases (96.1 to 100% similarity). No heteroduplexes or chimeras were found among the excised bands.

Seven bands (1 to 5, 9 and 13) were related to clones within the Bacteroidetes phylum from various marine waters (Table 2). Interestingly, 3 of these bands (1, 3 and 9) were observed exclusively at intermediate depths (25 to 100 m), while 4 bands (2, 4, 5 and 13) were dominant exclusively in samples from 200 to 300 m

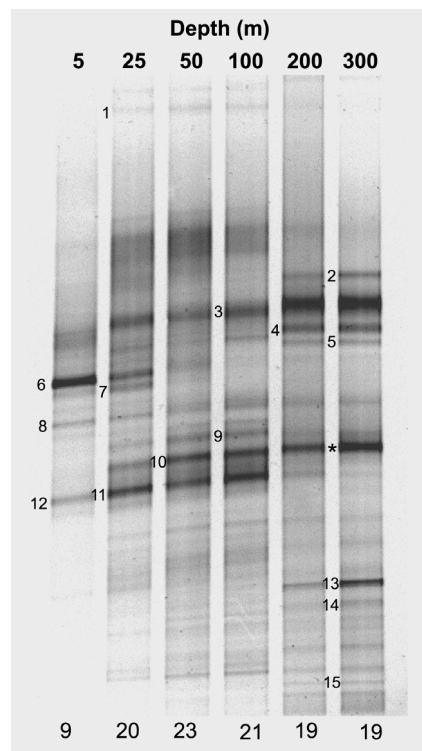


Fig. 5. Bacterial community composition profiles of samples from various depths. A denaturing gradient top to bottom of 29 to 52% was applied. The total number of discernible bands in each sample is shown below the gel. Excised and sequenced bands are numbered to the left of the lane. \*Excised band with the same vertical position as band 10. The relationships of excised band sequences to other sequences in the GenBank database are shown in Table 2

depth. Bands 2 and 4 showed a high similarity (>97%) to clones from an estuary (Northeastern Massachusetts, Acinas et al. 2004), while bands 1, 3, 5 and 9 were related to sequences obtained from various marine localities. The nearest relatives of bands 5 and 9 (94.4% and 96.1% similarity, respectively) were sequences obtained from the northern part of the North Sea during a coccolithophore bloom (Zubkov et al. 2002) and from the British part of the North Sea. Band 13 was only distantly related (90.4%) to a sequence obtained from a diatom culture (Schäfer et al. 2002).

Three bands (6 to 8) were related to photosynthetic organisms and were exclusively found down to 25 m depth. While bands 6 and 7 were almost identical to a cyanobacterial and a eukaryotic clone, respectively, band 8 was identical to a plastid from *Dinophysis norvegica* (Takishita et al. 2005). This plastid has recently been shown to be a so-called kleptoplastid originating from the cryptophyte *Teleaulax amphiox-ia* (Janson 2004). Both *Dinophysis* spp. and cryptophytes were observed microscopically in our samples (data not shown).

Table 2. Nearest relatives of the sequenced DGGE bands according to Blast 2.2.10 (February 2005). Taxonomy: Taxonomic affiliation as reported in GenBank

Name	Similarity (%)	Alignment <sup>a</sup>	Name	Nearest relative Origin	Depth	Taxonomy	Accession no. <sup>b</sup>
Band 1	98.0	548/548	Clone PI_4j12f	Estuary, Massachusetts	Not reported	Bacteroidetes	AY580583
Band 2	97.4	543/551	Clone 97A-17	Arctic Ocean	55 m	Bacteroidetes	AF354617
Band 3	98.2	552/552	Clone MB11E04	Monterey Bay, Pacific Ocean	Surface	Bacteroidetes	AY033305
Band 4	97.6	415/537	Clone PI_RT311	Estuary, Massachusetts	Not reported	Bacteroidetes	AY580639
Band 5	94.4	523/551	Clone ZD0255	North Sea	0 – 50 m, integrated	Bacteroidetes	AJ400343
Band 6	98.1	486/547	Clone SIMO-2124	Dean Creek, Georgia	Marsh sediment	Cyanobacteria	AY711490
Band 7	99.1	529/529	Clone JL-ECS-D119	Coastal East China Sea	Not reported	Plastid	AY663932
Band 8	100.0	520/529	<i>Dinophysis norvegica</i>	Okkirai Bay, Japan	0 – 20 m	Plastid	AB073116
Band 9	96.1	515/550	Clone BN_34	North Sea	Surface	Bacteroidetes	AY550843
Band 10	99.6	549/549	Clone PI_4z6d	Estuary, Massachusetts	Not reported	$\gamma$ -Proteobacteria	AY580767
Band 11	99.8	524/524	Clone F4C74	Antarctica	Not reported	$\alpha$ -Proteobacteria	AY697922
Band 12	97.7	533/533	Clone DC11-80-2	North Sea (Weser Estuary)	Not reported	$\alpha$ -Proteobacteria	AY145625
Band 13	90.4	405/561	Clone SB-39-TW	Diatom culture	Not reported	Bacteroidetes	AJ319833
Band 14	97.9	528/528	Clone JL-ETNP-z25	Eastern tropical north, Pacific Ocean	1000 m	$\delta$ -Proteobacteria	AY726934
Band 15	98.1	535/536	Clone arctic 95C-5	Arctic Ocean	55 m	$\delta$ -Proteobacteria	AF355039

<sup>a</sup>Part of the total sequence used in alignment. Primers were not included in the phylogenetic analyses

<sup>b</sup>Nucleotide sequences can be accessed via <http://www.ncbi.nlm.nih.gov/Entrez/>

Band 10, which was seen as a bright band at all depths except at the surface, was >99% identical to a  $\gamma$ -Proteobacteria clone from an estuary (Acinas et al. 2004). Bands 11 and 12 were related to sequences affiliated with the Roseobacter clade of  $\alpha$ -Proteobacteria. Band 11 appeared as a dominant band at 25 to 100 m depth and was almost identical to a sequence from Antarctica. Band 12, which had almost the same vertical position in the gel as Band 11, was closely related (97.7%) to a clone from the German Bight, North Sea (Selje et al. 2004). Both bands were also closely related (99.6% and 97.7%, respectively) to sequences obtained from the central North Sea during a coccolithophorid bloom (Gonzalez et al. 2000).

Bands 14 and 15 were found solely at 200 to 300 m and were closely related to  $\delta$ -Proteobacteria clones from the Pacific (1000 m) and Arctic (55 m) Oceans (Bano & Hollibaugh 2002). These sequences cluster within the so-called Marine Group B/SAR324 clade, which are proportionally most abundant in the aphotic zone of the Atlantic and Pacific Oceans (Fuhrman et al. 1993, Wright et al. 1997) and the North Sea (Gonzalez et al. 2000).

### Diurnal study

We examined whether the vertical migration of *Periphylla periphylla* from depth to the surface had an immediate effect on microbial activity at 5 m (Fig. 6). The stability of salinity and temperature at 5 m depth during the 24 h study (cf. Fig. 1) suggested that vertical mixing was negligible. While *P. periphylla* exhibited a clear diel migration pattern (Figs. 2 & 6), visual inspection revealed no apparent cyclic patterns over the 24 h period at 5 m for any of the other variables (Fig. 6). To quantify possible diel differences, data were grouped into night and day based on hours of light (Fig. 6) and tested for differences with a Mann-Whitney *U*-test. Except for *P. periphylla*, there were no significant differences between day and night in any of the variables (all *p*-values >0.05).

Bacterial community composition as obtained from sampling at times 07:00, 13:00, 19:00 and 01:00 h was stable. Only minor differences in the relative brightness of bands were detected and no differences in the presence or absence of bands were discernible (data not shown).

### DISCUSSION

Theoretically, direct release of DOC (Hansson & Norrman 1995) and nutrients (Schneider 1989, Nemazie et al. 1993) from jellyfishes, combined with the

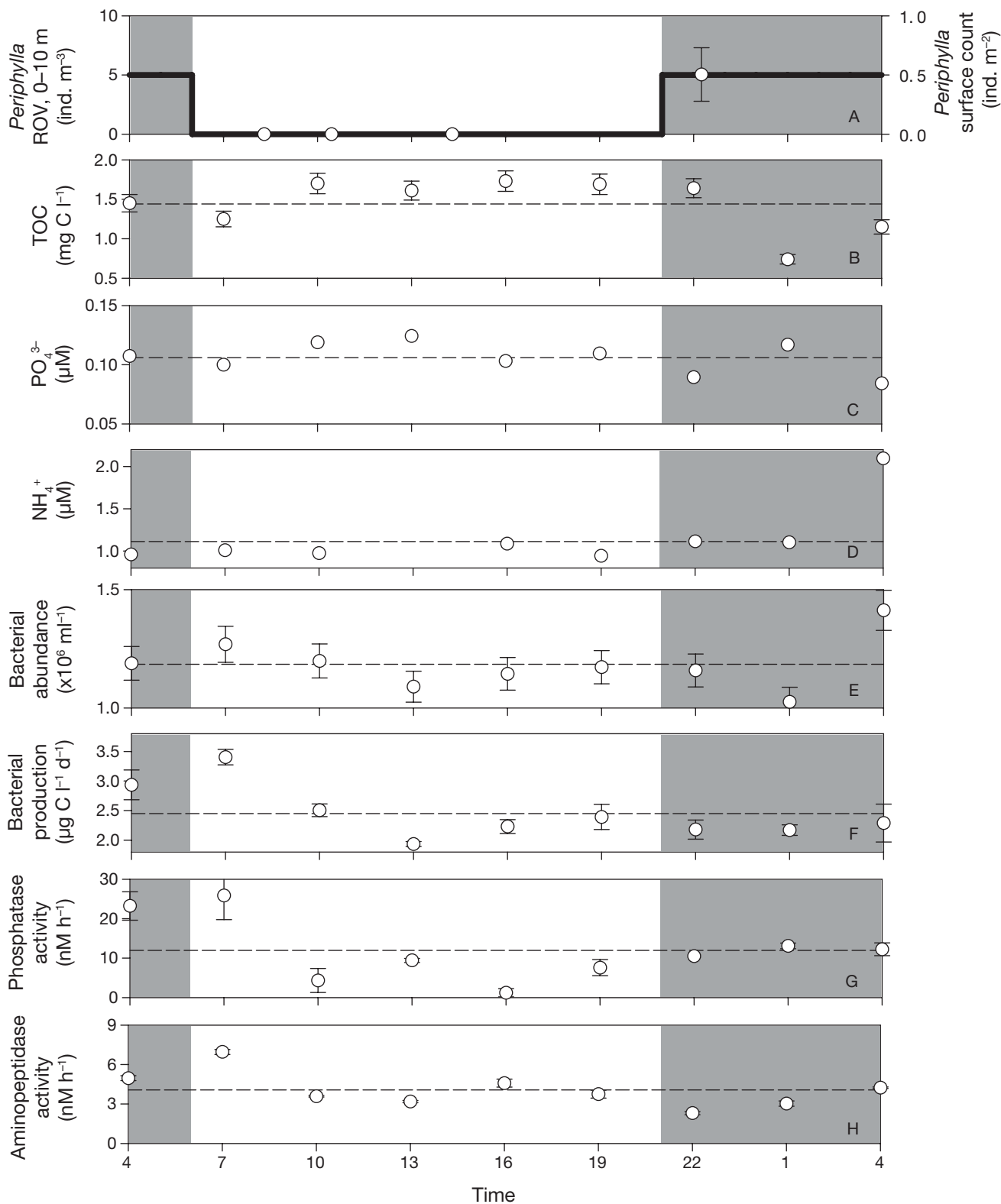


Fig. 6. *Periphylla periphylla*. Summary of the 24 h study at 5 m depth. (A) concentrations (open symbols) between 0 and 10 m as determined from ROV transects. The symbol indicates the mean concentration, error bars the min and the max, when using the 2 conversion factors (see 'Materials and methods'). Overlaid thick line shows surface counts (m<sup>-2</sup>). (B) Total organic carbon (TOC) concentrations; (C & D) nutrients concentrations; (E) bacterial abundance; (F) bacterial production; (G & H) ectoenzymatic activities. Data are mean  $\pm$  SD. Grey shading indicates dark hours, with sunrise at 06:00 h, and sunset at 21:16 h

re-structuring impact of jellyfish predation on higher trophic levels (Olesen 1995, Purcell & Arai 2001, Stibor et al. 2004) should affect bacterial growth conditions through changes in substrate quantity and quality. Hence, changes in bacterial community composition would be expected (Martinez et al. 1996). Here, we used Lurefjorden as a model of a jellyfish dominated system to examine effects of a large vertically migrating jellyfish population on microbial abundance, activity and community composition *in situ*. In an accompanying study, we demonstrated that dead *Periphylla periphylla* may stimulate as well as inhibit growth of various bacterial species (Titelman et al. 2006).

### Coupling between jellyfish, TOC and bacterial activity at depth?

Given the >15 h of daylight at the time of sampling, >50 % of the *Periphylla periphylla* biomass was located at 200 to 300 m depth when integrating over a day (Fig. 2D). Interestingly, the depth of minimum *P. periphylla* concentrations coincided with the TOC minimum. We attribute the subsurface elevated levels in TOC to the large *P. periphylla* biomass at depth, as we can rule out alternative explanations related to mixing and activities of other biota. Marine subsurface maxima of TOC resulting from a deep mixing event have been observed in the Sargasso Sea (Carlson et al. 1994). For Lurefjorden mixing is an unlikely explanation for the mid-water TOC minimum and elevated TOC levels at depth, as water exchange is restricted primarily to the layer above the sill, while the rest of the water column is vertically stable (sill depth = 20 m; Youngbluth & Båmstedt 2001, Sørnes 2005). *P. periphylla* dominates the pelagic biomass in Lurefjorden. The number of jellyfish was recently estimated from 4 yr of surveying to be  $0.4 \pm 0.25 P. periphylla \text{ m}^{-3} \text{ year}$  round (Sørnes 2005). The biomass of other biota, whose activities could potentially contribute to the TOC pool (e.g. Møller et al. 2003), is generally insignificant in the deeper parts of Lurefjorden (Figs. 1 & 3; Båmstedt & Youngbluth 2001, Sørnes 2005).

The combination of only 3 discrete TOC sampling depths, which were not influenced by phytoplankton productivity (100, 200 and 300 m), and a continuous profiling of *Periphylla periphylla* with 2 distinct peaks hamper statistical analyses; correlations between *P. periphylla* biomass and TOC are not significant at such large depth intervals (and low n). However, interpolation and subdividing into 20 m intervals yielded a significant correlation between TOC and *P. periphylla* between 80 and 260 m, i.e. at depths around and below the minimum TOC (see 'Results'). It is not surprising that TOC and *P. periphylla* profiles do not correlate

perfectly at large depths, as the resolution of the TOC sampling was much lower than that of the *P. periphylla* sampling; i.e. there are no TOC samples from the *P. periphylla* peak. Also, the amplitude of the *P. periphylla* migration varies with season with deeper distribution in autumn (Sørnes 2005), which may influence the TOC distribution at greater depths.

The pattern of a TOC minimum at ~100 to 150 m with increasing levels towards the bottom was accompanied by quantitatively similar patterns in bacterial production and ectoenzymatic activities. Bacterial activities were higher at 200 to 300 m relative to those at 100 m depth. This is in contrast to the North Atlantic, where bacterial production and enzyme activity decrease steadily with depth (0 to 300 m, Hoppe et al. 1993). Here we observed significant correlations between TOC and measures of bacterial activity. Hence, it is tempting to speculate that the elevated bacterial activity with depth in Lurefjorden is due to readily accessible carbon released by the *Periphylla periphylla*. Hansson & Norrman (1995) found that the jellyfish *Aurelia aurita* stimulated bacterial growth by releasing  $\sim 1 \text{ mg DOC ind.}^{-1} \text{ d}^{-1}$ . They speculated that this release may be quantitatively important in semi-enclosed systems with many jellyfish (Hansson & Norrman 1995). Physiological differences between *P. periphylla* and *A. aurita* may bias attempts to calculate the release of DOC from *P. periphylla*, as may the wide size variation in *P. periphylla* (0.05 to 2000 g, Sørnes 2005). However, directly applying the weight normalized release rate of *A. aurita* ( $0.012 \text{ mg C [g wet weight jellyfish]}^{-1} \text{ d}^{-1}$ ; Hansson & Norrman 1995), *P. periphylla* ROV concentrations of  $0.75 \text{ m}^{-3}$ , and a mean wet weight of 84 g (Table 1) suggest release rates of  $\sim 0.8 \text{ mg C m}^{-3} \text{ d}^{-1}$  in the layers of high *P. periphylla* abundance. The persistent *P. periphylla* population, in combination with the limited water exchange in Lurefjorden (Sørnes 2005), may thus contribute substantially to the DOC pool at depth on a yearly basis. In an accompanying paper, we found that dead *P. periphylla* leak TOC at rates as high as  $0.5 \text{ mg C (g wet weight jellyfish)}^{-1} \text{ d}^{-1}$  (Titelman et al. 2006).

### Bacterial community composition

To our knowledge, the DGGE and 16S rDNA analyses performed here provide the first information available on bacterial community composition from a marine system consistently dominated by jellyfish. The number of discernible bands was from 9 to 23, which is well within the range usually reported for marine waters (e.g. Fandino et al. 2001, Riemann & Middelboe 2002). The most striking findings from the analyses were (1) the profound dominance of phylotypes within

Bacteroidetes, (2) the pronounced differences in composition with depth, and (3) the presence of several phylotypes exclusively at 200 to 300 m depth.

Of the 15 different sequenced bands, 7 were related to Bacteroidetes clones previously obtained from marine waters. In a recent comparison of fluorescent *in situ* hybridization and DGGE, Castle & Kirchman (2004) found that their DGGE approach adequately sampled members of Bacteroidetes. Hence, although only some of the discernible DGGE bands were sequenced, we conclude that a large fraction of the bacterial community in Lurefjorden consisted of members of Bacteroidetes. Members of this phylum are generally among the most abundant marine bacteria (reviewed by Kirchman 2002) and are believed to specialize in particle colonization and degradation (DeLong et al. 1993, Riemann et al. 2000). More recently, findings of Bacteroidetes as important free-living organisms (e.g. Fandino et al. 2001) preferring polymeric substrates (Cottrell & Kirchman 2000) suggest that they might be specialized in degradation and uptake of high molecular weight DOM (Kirchman 2002). Lurefjorden is characterized by a high light attenuation coefficient, i.e. the light absorbance at 200 m is 2 to 3 times higher than in nearby fjords (Eiane et al. 1999). The dark environment favors jellyfish over fish, which are generally lacking in Lurefjorden (Eiane et al. 1999, Aksnes et al. 2004). Lurefjorden is less saline than neighboring fjords, and the water is partly of coastal origin (from the Baltic Sea and the rivers entering the North Sea) (Eiane et al. 1999). Members of Bacteroidetes are particularly efficient consumers of riverine DOM (Kisand & Wikner 2003). Hence, we hypothesize that the dominance of Bacteroidetes in Lurefjorden stems from prevailing substrate conditions governed by a combination of the coastal origin of the basin water and *Periphylla periphylla*.

Several dominant bacterial phylotypes were found solely in deep water. Four phylotypes (Bands 2, 4, 5 and 13) within Bacteroidetes were only observed in samples from 200 to 300 m depth. Of these bands, 5 and 13 were only distantly related to sequences in GenBank (94.4 and 90.4% similarity, respectively) suggesting that they might represent hitherto unknown species. Two other phylotypes (Bands 14 and 15) found at 200 to 300 m depth were related to the  $\delta$ -Proteobacteria Marine Group B/SAR324 cluster (Wright et al. 1997). The SAR324 cluster was vertically stratified in the water columns of both the Atlantic and Pacific Oceans with maxima between 160 and 500 m (Wright et al. 1997). A similar vertical distribution was found in the North Atlantic (Gonzalez et al. 2000). Hence, the 2 phylotypes belong to a phylogenetic group, which may be functionally specialized for life in the deep sea (Wright et al. 1997).

The depth-specific distribution of a significant number of bacterial phylotypes in Lurefjorden may be caused by the distribution of jellyfish through direct or indirect effects on microbial growth and/or mortality. As judged from bacterial abundance and production (Fig. 4), bacterial mortality increased with depth. Presumably, this was not caused by increased viral lysis with depth as virus:bacteria ratios were stable throughout the water column. The abundance of heterotrophic flagellates was low near the surface (<200 ml<sup>-1</sup>, not shown); however, flagellates, taking advantage of the limited grazing pressure from ciliates, could potentially increase in concentration with depth. Flagellate grazing, although sometimes assumed unselective, has the potential to affect bacterial community composition (Šimek et al. 1999). Gel-analyses-based observations of specific bacterial phylotypes associated with deeper waters, e.g. in the Arabian Sea (Riemann et al. 1999) and Antarctic coastal waters (Murray et al. 1998), suggest that environmental conditions associated with increased depth are generally highly selective. Thus, the presence of specific bacterial phylotypes at 200 to 300 m depth in Lurefjorden may be influenced by other factors than the conspicuous presence of a large biomass of *Periphylla periphylla* and the associated high levels of TOC.

Two bands were closely related to sequences within a recently defined cluster of the  $\alpha$ -Proteobacteria *Roseobacter* clade (Selje et al. 2004). Members of this cluster occur in many marine temperate and polar regions and account for ~10% of total bacteria in the German Bight, North Sea (Selje et al. 2004 and references therein). The presence of these bacteria in Lurefjorden is not surprising given the water exchange with the North Sea.

#### Diel effect of jellyfish in surface waters?

The microbial abundance and activity near the surface did not appear to be altered by a high abundance of *Periphylla periphylla*. Conceivably, the carbon released from *P. periphylla* was masked by other sources of bioavailable carbon, e.g. phytoplankton and copepod biomass and activity. Near the surface, the *P. periphylla* biomass at night was approximately half that of copepods, which did not migrate vertically. The DOM provided by copepods and their sloppy feeding (Møller et al. 2003) may be of better quality than DOM released from jellyfish. Similarly, the bacterial community analyses showed no diurnal signal in composition (data not shown). Although the bacterial community grew slowly (doubling time of up to 10 d; abundance divided by daily production; data not shown) single bacterial species may grow >5 times faster than the average

community (Pinhassi et al. 1999). Hence, changes in bacterial community composition in response to substrate provided by the migrating *P. periphylla* population were theoretically possible on a 24 h scale.

## CONCLUSION

Here, we examined microbial activity and community composition in a natural marine system where jellyfish dominates biomass. At depth the jellyfish seemed to stimulate microbial activity, while this could not be demonstrated near the surface. Generally, jellyfish, TOC and bacterial activity measures all had minima at mid-depth and increasing values towards the bottom. The coinciding vertical patterns of jellyfish biomass and TOC at depth indicate a possible leakage of organic matter from jellyfish tissue or feeding activity. The increase in TOC levels at depth was in turn correlated with increased bacterial activities. Several bacterial phylotypes were specifically found at the depths with highest jellyfish biomass, possibly reflecting bacterial functional adaptations to the local substrate regime. In an accompanying paper we show that *Periphylla periphylla* may indeed both stimulate and retard bacterial growth suggesting a release of both substrate and inhibitory compounds, as well as a possible impact on bacterial community composition (Titelman et al. 2006). Thus, *P. periphylla* has the potential to affect bacteria, but a causal link between the depth-specific bacterial phylotypes and the jellyfish *P. periphylla* cannot be unambiguously established from these field data. Nevertheless, we suggest that jellyfish proliferations may directly and indirectly affect trophic levels down to microbes in the pelagic foodweb.

**Acknowledgements.** We thank P. Griekspoor for technical assistance in sequencing analyses, C. Legrand for advice on ciliate and phytoplankton examinations, T. Nilsen, J. E. Skjæraasen and C. Legrand for discussions on statistics, and the crew of RV 'Haakon Mosby' for help with sampling. Nutrient and TOC were analysed at Umeå Marine Science Centre. T. Sørnes kindly commented on an earlier draft. We also thank the reviewers for constructive comments. This work formed part of the EUROGEL project funded by the European Commission (EVK3-CT-2002-00074; U.B., J.T.). Additional financial support was given by FORMAS (2004-2539; L.R., J.T.).

## LITERATURE CITED

- Acinas SG, Klepac-Ceraj V, Hunt DE, Pharino C, Ceraj I, Distel DL, Polz MF (2004) Fine-scale phylogenetic architecture of a complex bacterial community. *Nature* 430:551–554
- Aksnes DL, Nejstgaard J, Sædberg E, Sørnes T (2004) Optical control of fish and zooplankton populations. *Limnol Oceanogr* 49:233–238
- Altschul SF, Gish W, Miller W, Myers EW, Lipman DJ (1990) Basic local alignment search tool. *J Mol Biol* 215:403–410
- Bano N, Hollibaugh JT (2002) Phylogenetic composition of bacterioplankton assemblages from the Arctic Ocean. *Appl Environ Microbiol* 68:505–518
- Berggreen U, Hansen B, Kiørboe T (1988) Food size spectra, ingestion and growth of the copepod *Acartia tonsa* during development: implications for determination of copepod production. *Mar Biol* 99:341–352
- Bjørnsen PK (1988) Phytoplankton exudation of organic matter: Why do healthy cells do it? *Limnol Oceanogr* 33:151–154
- Boström KH, Simu K, Hagström Å, Riemann L (2004) Optimization of DNA extraction for quantitative marine bacterioplankton community analysis. *Limnol Oceanogr Methods* 2:365–373
- Carlson CA, Ducklow HW, Michaels AF (1994) Annual flux of dissolved organic carbon from the euphotic zone in the northwestern Sargasso Sea. *Nature* 371:405–408
- Castle D, Kirchman DL (2004) Composition of estuarine bacterial communities assessed by denaturing gradient gel electrophoresis and fluorescence *in situ* hybridization. *Limnol Oceanogr Methods* 2:303–314
- Cole JR, Chai B, Marsh TL, Farris RJ and 7 others (2003) The Ribosomal Database Project (RDP-II): previewing a new autoaligner that allows regular updates and the new prokaryotic taxonomy. *Nucleic Acids Res* 31(1):442–443
- Cottrell MT, Kirchman DL (2000) Natural assemblages of marine Proteobacteria and members of the *Cytophaga-Flavobacter* cluster consuming low- and high-molecular-weight dissolved organic matter. *Appl Environ Microbiol* 66:1692–1697
- DeLong EF, Franks DG, Alldredge AL (1993) Phylogenetic diversity of aggregate-attached vs. free-living marine bacterial assemblages. *Limnol Oceanogr* 38:924–934
- Eiane K, Aksnes DL, Bagøien E, Kaartvedt S (1999) Fish or jellies—a question of visibility? *Limnol Oceanogr* 44:1352–1357
- Fandino LB, Riemann L, Steward GF, Long RA, Azam F (2001) Variations in bacterial community structure during a dinoflagellate bloom analyzed by DGGE and 16S rDNA sequencing. *Aquat Microb Ecol* 23:119–130
- Fuhrman JA, Azam F (1982) Thymidine incorporation as a measure of heterotrophic bacterioplankton production in marine surface waters: evaluation and field results. *Mar Biol* 66:109–120
- Fuhrman JA, McCallum K, Davis AA (1993) Phylogenetic diversity of subsurface marine microbial communities from the Atlantic and Pacific Oceans. *Appl Environ Microbiol* 59:1294–1302
- Gasol JM, del Giorgio PA (2000) Using flow cytometry for counting natural planktonic bacteria and understanding the structure of planktonic bacterial communities. *Sci Mar* 64:197–224
- Gonzalez JM, Simó R, Massana R, Covert JS, Casamayor EO, Pedrós-Alio C, Moran MA (2000) Bacterial community structure associated with a dimethylsulfoniopropionate-producing North Atlantic algal bloom. *Appl Environ Microbiol* 66:4237–4246
- Grasshoff K, Ehrhardt M, Kremling K (1983) *Methods of seawater analysis*. Verlag Chemie, Weinheim
- Hansson LJ, Norrman B (1995) Release of dissolved organic carbon (DOC) by the scyphozoan jellyfish *Aurelia aurita* and its potential influence on the production of planktonic bacteria. *Mar Biol* 121:527–532
- Hoppe HG, Ducklow H, Karrasch B (1993) Evidence for dependency of bacterial growth on enzymatic hydrolysis of particulate organic matter in the mesopelagic ocean. *Mar Ecol Prog Ser* 93:277–283
- Janson S (2004) Molecular evidence that plastids in the toxin-producing dinoflagellate genus *Dinophysis* originate from

- the free-living cryptophyte *Teleaulax amphioxeia*. Environ Microbiol 6:1102–1106
- Kirchman DL (2002) The ecology of *Cytophaga-Flavobacteria* in aquatic environments. FEMS Microbiol Ecol 1317:1–10
- Kisand V, Wikner J (2003) Combining culture-dependent and independent methodologies for estimation of richness of estuarine bacterioplankton consuming riverine dissolved organic matter. Appl Environ Microbiol 69:3607–3616
- Lee SH, Fuhrman JA (1987) Relationships between biovolume and biomass of naturally derived marine bacterioplankton. Appl Environ Microbiol 53:1298–1303
- Lynam CP, Hay SJ, Brierley AS (2004) Interannual variability in abundance of North Sea jellyfish and links to the North Atlantic Oscillation. Limnol Oceanogr 49:637–643
- Martinez J, Smith DC, Steward GF, Azam F (1996) Variability in ectohydrolytic enzyme activities of pelagic marine bacteria and its significance for substrate processing in the sea. Aquat Microb Ecol 10:223–230
- Menden-Deuer S, Lessard EJ (2000) Carbon to volume relationships for dinoflagellates, diatoms, and other protist plankton. Limnol Oceanogr 45:569–579
- Mills CE (2001) Jellyfish blooms: Are populations increasing globally in response to changing ocean conditions? Hydrobiol 451:55–68
- Møller EF, Thor P, Nielsen TG (2003) Production of DOC by *Calanus finmarchicus*, *C. glacialis*, and *C. hyperboreus* through sloppy feeding and leakage from fecal pellets. Mar Ecol Prog Ser 262:185–191
- Murray AE, Preston CM, Massana R, Taylor LT, Blakis A, Wu K, DeLong EF (1998) Seasonal and spatial variability of bacterial and archaeal assemblages in the coastal waters near Anvers Island, Antarctica. Appl Environ Microbiol 64:2585–2595
- Muyzer G, De Waal EC, Uitterlinden AG (1993) Profiling of complex microbial populations by denaturing gradient gel electrophoresis analysis of polymerase chain reaction-amplified genes coding for 16S rRNA. Appl Environ Microbiol 59:695–700
- Muyzer G, Brinkhoff T, Nübel U, Santegoeds CM, Schäfer H, Wawer C (1998) Denaturing gradient gel electrophoresis (DGGE) in microbial ecology. In: Akkermans ADL, van Elsas JD, De Bruin FJ (eds) Molecular microbial ecology manual. Kluwer Academic Publishers, London, Section 344:1–27
- Nemazie DA, Purcell JE, Glibert PM (1993) Ammonium excretion by gelatinous zooplankton and their contribution to the ammonium requirements of microplankton in Chesapeake Bay. Mar Biol 116:451–458
- Noble RT, Fuhrman JA (1998) Use of SYBR Green I for rapid epifluorescence counts of marine viruses and bacteria. Aquat Microb Ecol 14:113–118
- Olesen NJ (1995) Clearance potential of jellyfish *Aurelia aurita*, and predation impact on zooplankton in a shallow cove. Mar Ecol Prog Ser 124:63–72
- Pinhassi J, Azam F, Hemphälä J, Long RA, Martinez J, Zweifel UL, Hagström Å (1999) Coupling between bacterioplankton species composition, population dynamics, and organic matter degradation. Aquat Microb Ecol 17:13–26
- Priddle J, Whitehouse MJ, Ward P, Shreeve RS and 5 others (2003) Biogeochemistry of a Southern Ocean plankton ecosystem: using natural variability in community composition to study the role of metazooplankton in carbon and nitrogen cycles. J Geophys Res 108 (C4):no. 8082
- Purcell JE, Arai MN (2001) Interactions of pelagic cnidarians and ctenophores with fish: a review. Hydrobiol 451:27–44
- Rey-Rassat C, Bonnet D, Irigoien X, Harris R, Head R, Carlotti F (2004) Is weight an important parameter when measuring copepod growth? J Exp Mar Biol Ecol 313:19–27
- Riemann L, Middelboe M (2002) Stability of bacterial and viral community compositions in Danish coastal waters as depicted by DNA fingerprinting techniques. Aquat Microb Ecol 27:219–232
- Riemann L, Winding A (2001) Community dynamics of free-living and particle-associated bacterial assemblages during a freshwater phytoplankton bloom. Microb Ecol 42:274–285
- Riemann B, Bjørnsen PK, Newell S, Fallon R (1987) Calculation of cell production of coastal marine bacteria based on measured incorporation of (<sup>3</sup>H)thymidine. Limnol Oceanogr 32:471–476
- Riemann L, Steward GF, Fandino LB, Campbell L, Landry MR, Azam F (1999) Bacterial community composition during two consecutive NE Monsoon periods in the Arabian Sea studied by denaturing gradient gel electrophoresis (DGGE) of rRNA genes. Deep-Sea Res II 46:1791–1811
- Riemann L, Steward GF, Azam F (2000) Dynamics of bacterial community composition and activity during a mesocosm diatom bloom. Appl Environ Microbiol 66:578–587
- Sabatini M, Kiørboe T (1994) Egg production, growth and development of the cyclopid copepod *Oithona similis*. J Plankton Res 16:1329–1351
- Schneider G (1989) The common jellyfish, *Aurelia aurita*: standing stock, excretion and nutrient regeneration in the Kiel Bight, Western Baltic. Mar Biol 100:507–514
- Schäfer H, Abbas B, Witte H, Muyzer G (2002) Genetic diversity of 'satellite' bacteria present in cultures of marine diatoms. FEMS Microbiol Ecol 42:25–35
- Selje N, Simon M, Brinkhoff T (2004) A newly discovered *Roseobacter* cluster in temperate and polar oceans. Nature 427:445–448
- Šimek K, Kojecká P, Nedoma J, Hartman P, Vrba J, Dolan J (1999) Shifts in bacterial community composition associated with different microzooplankton size fractions in a eutrophic reservoir. Limnol Oceanogr 44:1634–1644
- Sørnes TA (2005) Visual or tactile zooplanktonvores—structuring effects of the underwater visual environment. PhD thesis, University of Bergen, Bergen
- Stibor H, Vadstein O, Diehl S, Gelzleichter A and 10 others (2004) Copepods act as a switch between alternative trophic cascades in marine pelagic food webs. Ecol Lett 7:321–328
- Takishita K, Kazuhiko K, Maruyama T, Ogata T (2005) Molecular evidence for plastid robbery (kleptoplastidy) in *Dinophysis*, a dinoflagellate causing diarrhetic shellfish poisoning. Protist 153:293–302
- Titelman J, Riemann L, Sørnes TA, Nilsen T, Griekspoor P, Båmstedt U (2006) Turnover of dead jellyfish: stimulation and retardation of microbial activity. Mar Ecol Prog Ser 325:43–58
- Wen K, Ortmann AC, Suttle CA (2004) Accurate estimation of viral abundance by epifluorescence microscopy. Appl Environ Microbiol 70:3862–3867
- Wintzingerode FV, Göbel UB, Stackebrandt E (1997) Determination of microbial diversity in environmental samples: pitfalls of PCR-based rRNA analysis. FEMS Microb Rev 21:213–229
- Wright TD, Vergin KL, Boyd PW, Giovannoni SJ (1997) A novel delta-subdivision proteobacterial lineage from the lower ocean surface layer. Appl Environ Microbiol 63:1441–1448
- Youngbluth MJ, Båmstedt U (2001) Distribution, abundance, behavior and metabolism of *Periphylla periphylla*, a mesopelagic coronate medusa in a Norwegian fjord. Hydrobiol 451:321–333
- Zubkov MV, Fuchs BM, Archer SD, Kiene RP, Amann R, Burkill PH (2002) Rapid turnover of dissolved DMS and DMSP by defined bacterioplankton communities in the stratified euphotic zone of the North Sea. Deep-Sea Res II 49:3017–3038